Square vortex lattices for two-component superconducting order parameters

D. F. Agterberg
Theoretische Physik, Eidgenössiche Technische Hochschule-Hönggerberg, 8093 Zürich, Switzerland
(Received 25 June 1998)

I investigate the vortex lattice structure of the Ginzburg-Landau free energy for a two component order parameter in the weak-coupling clean limit when the field is along the high-symmetry axis in a tetragonal crystal. It is shown that the vortex-lattice phase diagram as a function of the Ginzburg-Landau free-energy parameters includes phases with a hexagonal, centered rectangular, rectangular, and square unit cells. It is also shown that the square vortex lattice has the largest region of stability. The field distribution of the square vortex lattice near H_{c2} is determined and the application of this model to Sr_2RuO_4 is discussed.
[S0163-1829(98)00845-5]

The oxide Sr_2RuO_4 has a structure similar to high-T_c materials and was discovered to be superconducting with a $T_c=1.35$ K by Maeno *et al.* in 1994.[1] It has been established that this superconductor is not a conventional *s*-wave superconductor: NQR measurements show no indication of a Hebel-Slichter peak in $1/T_1T$,[2] T_c is strongly suppressed by nonmagnetic impurities,[3] and tunneling experiments are inconsistent with *s*-wave pairing.[4] More recently there have been two experimental results that shed more light on the nature of the superconducting state. The μSR experiments of Luke *et al.* indicate that the superconducting state *breaks* time reversal symmetry, which implies that the superconducting order parameter must have more than one component.[5] Of the possible representations (reps) of the D_{4h} point group, the two-dimensional (2D) Γ_{5u} representation (rep) is the most likely state that exhibits this property. The order parameter in this case has two components (η_1,η_2) that share the same rotation-inversion symmetry properties as (k_x,k_y).[6] The broken $\mathcal{T}$ state would then correspond to $(\eta_1,\eta_2)\propto(1,i)$. Theoretical arguments supporting a triplet pairing state have been given in Ref. 7. Given that this material may well be described by such an order parameter, it is of interest to explore further consequences of a two-component order parameter. In an earlier work it was shown that a consequence of the low-temperature broken time reversal symmetry state is that the mean-field vortex lattice phase diagram will exhibit two vortex lattice phases when the field is along a high-symmetry direction in the basal plane.[8] Another important experimental development is the observation of a square vortex lattice in Sr_2RuO_4 by Riseman *et al.*[9] Within the context of the orbital-dependent superconductivity model for Sr_2RuO_4 the orientation of the square vortex lattice relative to the underlying ionic lattice dictates which of the Ru orbitals exhibits superconductivity.[8,10] This work focuses on the magnetic-field distribution and the structure of the vortex lattice for the field along the *c* axis for this two-component model.

The free energy for the Γ_{5u} representation of the tetragonal point group is given by[6]

$$
\begin{aligned}
f=&-\alpha|\vec{\eta}|^2+\beta_1|\vec{\eta}|^4/2+\beta_2(\eta_1\eta_2^*-\eta_2\eta_1^*)^2/2\\
&+\beta_3|\eta_1|^2|\eta_2|^2+\kappa_1(|\tilde{D}_x\eta_1|^2+|\tilde{D}_y\eta_2|^2)+\kappa_2(|\tilde{D}_y\eta_1|^2\\
&+|\tilde{D}_x\eta_2|^2)+\kappa_5(|\tilde{D}_z\eta_1|^2+|\tilde{D}_z\eta_2|^2)+\kappa_3[(\tilde{D}_x\eta_1)\\
&\times(\tilde{D}_y\eta_2)^*+\text{H.c.}]+\kappa_4[(\tilde{D}_y\eta_1)(\tilde{D}_x\eta_2)^*+\text{H.c.}]\\
&+h^2/(8\pi),
\end{aligned}
\tag{1}
$$

where $\alpha=\alpha_0(T-T_c)$, $\tilde{D}_j=\nabla_j-(2ie/\hbar c)A_j$, $\mathbf{h}=\nabla\times\mathbf{A}$, and $\mathbf{A}$ is the vector potential. To simplify the analysis the Ginzburg-Landau coefficients are determined within a weak-coupling approximation in the clean limit. The measurements of Mackenzie *et al.* of T_c as a function of impurity concentration show that the ratio of the mean free path to the zero-temperature coherence length is >8 for $T_c>1.3$ K (Ref. 3) indicating that the clean limit should be a reasonable approximation for Sr_2RuO_4. Without an experimental knowledge of the characteristic frequency of the boson responsible for the pairing (presumably ferromagnetic spin fluctuations) it cannot be determined that the weak-coupling limit is appropriate for Sr_2RuO_4. Note that the spin fluctuation theory of Mazin and Singh indicates that $T_c/T_P\approx10^{-2}$, where T_P is the characteristic paramagnon frequency.[11] This estimate in conjunction with $T_c/T_F\approx10^{-4}$ indicates that the weak-coupling approximation is reasonable for Sr_2RuO_4, but further experiments are required to ensure this. Taking for the Γ_{5u} rep the gap function described by the pseudo-spin-pairing gap matrix (note that this choice is not unique): $\hat{\Delta}=i[\eta_1v_x/(\langle v_x^2\rangle)^{1/2}+\eta_2v_y/(\langle v_x^2\rangle)^{1/2}]\sigma_z\sigma_y$ where the brackets $\langle\rangle$ denote an average over the Fermi surface and σ_i are the Pauli matrices, writing $\eta_+=(\eta_1+i\eta_2)/\sqrt{2}$, $\eta_-=(\eta_1-i\eta_2)/\sqrt{2}$, and rotating $(\tilde{D}_x,\tilde{D}_y)$ by an angle θ about the z axis to obtain $(\tilde{D}_{\tilde{x}},\tilde{D}_{\tilde{y}})$, the following dimensionless free energy is found:

$$
\begin{aligned}
f={}&-(|\eta_+|^2+|\eta_-|^2)+(|\eta_+|^4+|\eta_-|^4)/2+2|\eta_+|^2|\eta_-|^2+\nu[(\eta_-\eta_+^*)^2+(\eta_-^*\eta_+)^2]/2+|D_{\tilde{x}}\eta_+|^2+|D_{\tilde{y}}\eta_-|^2+|D_{\tilde{x}}\eta_-|^2\\
&+|D_{\tilde{y}}\eta_+|^2+(e^{i2\theta}+\nu e^{-i2\theta})[(D_{\tilde{x}}\eta_+)(D_{\tilde{x}}\eta_-)^*-(D_{\tilde{y}}\eta_+)(D_{\tilde{y}}\eta_-)^*]/2+(e^{-i2\theta}+\nu e^{i2\theta})[(D_{\tilde{x}}\eta_-)(D_{\tilde{x}}\eta_+)^*-(D_{\tilde{y}}\eta_-)\\
&\times(D_{\tilde{y}}\eta_+)^*]/2+I(e^{-i2\theta}-\nu e^{i2\theta})[(D_{\tilde{x}}\eta_-)(D_{\tilde{y}}\eta_+)^*+(D_{\tilde{y}}\eta_-)(D_{\tilde{x}}\eta_+)^*]/2-I(e^{i2\theta}-\nu e^{-i2\theta})[(D_{\tilde{x}}\eta_+)(D_{\tilde{y}}\eta_-)^*\\
&+(D_{\tilde{y}}\eta_+)(D_{\tilde{x}}\eta_-)^*]/2+\tilde{\kappa}_5(|D_z\eta_+|^2+|D_z\eta_-|^2)+h^2, \qquad (2)
\end{aligned}
$$

where $h=\nabla\times\mathbf{A}$, $D_\nu=\nabla_\nu/\kappa-iA_\nu$, f is in units $B_c^2/(4\pi)$, lengths are in units $\lambda=[\hbar^2c^2\beta_1/(32e^2\kappa_1\alpha\pi)]^{1/2}$, $\tilde{\kappa}_5=2\kappa_5/\kappa_{12}$, $\kappa_{12}=\kappa_1+\kappa_2=4\kappa_1/(3+\nu)$, $\nu=(\langle v_x^4\rangle-3\langle v_x^2v_y^2\rangle)/(\langle v_x^4\rangle+\langle v_x^2v_y^2\rangle)$, h is in units $\sqrt{2}B_c=\Phi_0/(2\pi\lambda\zeta)$ (here B_c has been chosen to represent the thermodynamic critical field), $\alpha=\alpha_0(T-T_c)$, $\xi=(\kappa_{12}/2\alpha)^{1/2}$, and $\kappa=\lambda/\xi$. The parameter ν (note $|\nu|\leqslant 1$) gives a measure of the square anisotropy of the Fermi surface. For a cylindrical Fermi surface $\nu=0$ and for a square Fermi surface $|\nu|=1$. It is easy to verify that in zero field $(\eta_1,\eta_2)\propto(1,i)$ is the stable ground state for $|\nu|\leqslant 1$.

For the magnetic field along the c axis the ground state is found by setting $D_z=0$. Writing $\Pi_+=\sqrt{\kappa}(iD_{\tilde{x}}+D_{\tilde{y}})/\sqrt{2H}$ and $\Pi_-=\sqrt{\kappa}(iD_{\tilde{x}}-D_{\tilde{y}})/\sqrt{2H}$, minimizing the quadratic portion of Eq. 2 with respect to η_+ and η_- yields

$$
\kappa\begin{pmatrix}\eta_+\\ \eta_-\end{pmatrix}=H\begin{pmatrix}1+2N & e^{-2i\theta}\Pi_+^2+\nu e^{2i\theta}\Pi_-^2\\ e^{2i\theta}\Pi_-^2+\nu e^{-2i\theta}\Pi_+^2 & 1+2N\end{pmatrix}\times\begin{pmatrix}\eta_+\\ \eta_-\end{pmatrix}, \qquad (3)
$$

where $N=\Pi_+\Pi_-$. The maximum value of the externally applied field H that allows a nonzero solution for (η_+,η_-) yields the upper critical field H_{c_2}. At $H=H_{c2}$ the vector potential is that for a spatially uniform field $\mathbf{A}=(0,Hx,0)$. Expanding (η_+,η_-) in terms of the eigenstates of N (Landau levels) up to $N=32$ and diagonalizing the resulting matrix yields the result for $e_H=\kappa/H_{c_2}$ shown as a function of ν in Fig. 1.

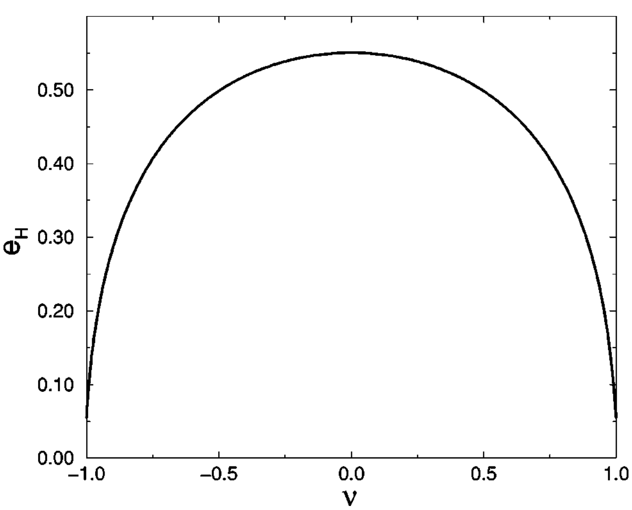

FIG. 1. $e_H=\kappa/H_{c_2}$ as a function of ν.

The form of the eigenstate of the H_{c_2} solution is found to be $\eta_+(\mathbf{r})=\Sigma_{n\geqslant 0}a_{4n+2}\phi_{4n+2}(\mathbf{r})$, and $\eta_-(\mathbf{r})=\Sigma_{n\geqslant 0}a_{4n}\phi_{4n}(\mathbf{r})$, where $\phi_n(\mathbf{r})$ are the harmonic oscillator wave functions (Landau levels). As is well known, these wave functions have a large degeneracy, and the form of the vortex lattice is found by including the nonlinear terms of the Ginzburg-Landau equations perturbatively to break this degeneracy. Following the procedure of Abrikosov, the average Gibbs free-energy density is found to be (a derivation of this result for unconventional superconductors can be found in Ref. 12 and for a mixed d- and s-wave order parameter in Ref. 13)

$$
\overline{g}=-H^2-\frac{(H_{c_2}-H)^2}{(2\tilde{\kappa}^2-1)\beta_A}, \qquad (4)
$$

where

$$
\beta_A=\frac{\overline{h_s^2}}{(\overline{h_s})^2}, \qquad (5)
$$

$$
2\tilde{\kappa}^2=\frac{\overline{f_4}}{\overline{h_s^2}}, \qquad (6)
$$

f_4 is the fourth-order homogeneous free energy, h_s is the field (along the c axis) induced by the supercurrent, and the overbar denotes a spatial average. The form of the vortex lattice is found by minimizing $(2\tilde{\kappa}^2-1)\beta_A$. To do this h_s must be found. By minimizing the Ginzburg-Landau free energy with respect to the vector potential the following relation is found for h_s:

$$
\begin{aligned}
j_+\equiv{}&\frac{\partial h_s}{\partial y}-i\frac{\partial h_s}{\partial x}\\
={}&\eta_+^*(\Pi_-\eta_+)+\eta_+(\Pi_+\eta_+)^*+\eta_-^*(\Pi_-\eta_-)\\
&+\eta_-(\Pi_+\eta_-)^*+e^{i2\theta}[\eta_-^*(\Pi_+\eta_+)+\eta_+(\Pi_-\eta_-)^*]\\
&+\nu e^{i2\theta}[\eta_+^*(\Pi_+\eta_-)+\eta_-(\Pi_-\eta_+)^*]
\end{aligned}
$$

$$
\begin{aligned}
j_-\equiv{}&\frac{\partial h_s}{\partial y}+i\frac{\partial h_s}{\partial x}=\eta_+(\Pi_-\eta_+)^*+\eta_+^*(\Pi_+\eta_+)\\
&+\eta_-(\Pi_-\eta_-)^*+\eta_-^*(\Pi_+\eta_-)+e^{-i2\theta}[\eta_-(\Pi_+\eta_+)^*\\
&+\eta_+^*(\Pi_-\eta_-)]+\nu e^{-i2\theta}[\eta_+(\Pi_+\eta_-)^*+\eta_-^*(\Pi_-\eta_+)] \qquad (7)
\end{aligned}
$$

Near H_{c_2} the field h_s is found by substituting the vector potential for the homogeneous field and the order parameter solution near H_{c_2} into the right-hand side of Eq. (7). Writing the left-hand side of Eq. 7 as $j_i=\Sigma_{n,m}(j_i)_{n,m}\phi_n\phi_m^*$ and writing $h_s=\Sigma_{n,m}h_{n,m}\phi_n\phi_m^*$ yields (see Ref. 14)

$$h_{l,l}=\sum_{n=l}^{\infty}(j_+)_{n+1,n}/\sqrt{n+1}, \tag{8}$$

$$h_{l,p}=[\sqrt{l}(j_+)_{l-1,p}-\sqrt{p}(j_+)^*_{p-1,l}]/(p-l), \quad l\neq p.$$

The form of β_A and $\tilde{\kappa}$ will therefore be determined by terms of the type $\phi_n(\mathbf{r})\phi_m^*(\mathbf{r})\phi_p(\mathbf{r})\phi_l^*(\mathbf{r})$. To evaluate such terms I make the assumption that the vortex lattice unit cell contains one flux quantum. The shape of the unit cell is kept arbitrary and the convention introduced by Saint-James *et al.*[15] to describe the unit cell is used. The lattice geometry is depicted in Fig. 2.

The lattice vectors are $\mathbf{a}_1=a(1,0)$ and $\mathbf{a}_2=b(\cos\alpha,\sin\alpha)$, with the single flux quantum constraint $ab\sin\alpha=2\pi$, where a and b are in units $l_H=\sqrt{\lambda\xi/H}$. This assumption allows the functions ϕ_n to be written as[12]

$$\phi_n(\mathbf{r})=2^{-n/2}\pi^{-1/4}(n!)^{-1/2}\times\sum_m c_m e^{i2\pi(m-1/2)x/a}e^{-(y-y_m)^2/2}H_n(y-y_m), \tag{9}$$

where $c_n=e^{i\pi n(\rho+1-n\rho)}$, $y_n=(n-1/2)\sqrt{2\pi\sigma}$, $\sigma=(b/a)\sin\alpha$, $\rho=(b/a)\cos\alpha$, and H_n are the Hermite polynomials. To evaluate β_A and $\tilde{\kappa}$ it is useful to express the spatial averages in terms of a sum over the reciprocal lattice of the vortex lattice. The reciprocal lattice is given by $\mathbf{G}=l_1\mathbf{k}_1+l_2\mathbf{k}_2$ where $\mathbf{k}_1=(2\pi/a\sin\alpha)(\sin\alpha,-\cos\alpha)$ $\mathbf{k}_2=(2\pi/b\sin\alpha)(1,0)$. The general form of β_A becomes

$$\beta_A=\frac{\sum_{n,m,p,l}a_{n,m,p,l}\sum_{l_1,l_2}\langle\phi_n\phi_m^*\rangle_{l_1,l_2}\langle\phi_p\phi_l^*\rangle_{-l_1,-l_2}}{\left[\sum_n a_n\langle|\phi_n|^2\rangle_{0,0}\right]^2}, \tag{10}$$

where the coefficients $a_{n,m,p,l}$ and a_n are determined by f_4, h_s, and the form of the eigenfunction near $H_{c_2}^c$, $\langle f\rangle_{l_1,l_2}=(ab\sin\alpha)^{-1}\int_{uc}e^{-i\mathbf{G}\cdot\mathbf{r}}f(\mathbf{r})$, and uc denotes the unit cell. The following relation makes this formulation for determining β_A and $\tilde{\kappa}$ useful (found using the addition theorem for Hermite polynomials):

$$\langle\phi_p\phi_m^*\rangle_{l_1,l_2}=\frac{\sqrt{p!m!}}{2^{m+p}}\langle|\phi_0|^2\rangle_{l_1,l_2}\times\sum_{r=0}^{p}\sum_{s=0}^{m}\frac{C_{r,s}H_{p-r}[-z_{l_1,l_2}]H_{m-s}[z^*_{l_1,l_2}]}{(p-r)!(m-s)!}, \tag{11}$$

where

$$C_{r,s}=\sum_{l=0}^{[r/2]}\sum_{p=0}^{[s/2]}(-1)^{l+p}\times\frac{(r+s-2l-2p)!2^{-l-p+(r+s)/2}}{(r-2l)!(s-2p)!l!p![(r+s)/2-l-p]!}, \tag{12}$$

$z_{l_1,l_2}=\sqrt{\pi}[l_1\sqrt{\sigma}+i(l_2-\rho l_1)/\sqrt{\sigma}]$, and

$$\langle|\phi_0|^2\rangle_{l_1,l_2}=\frac{\sqrt{\pi}}{b\sin\alpha}e^{i\pi(l_1+l_2+l_1l_2)}e^{-\pi\sigma l_1^2/2}e^{-\pi(l_2-l_1\rho)^2/2\sigma}. \tag{13}$$

The following relation is also useful:

$$\langle\phi_p\phi_0^*\rangle_{l_1,l_2}=[\sqrt{2}z_{l_1,l_2}]^p\langle|\phi_0|^2\rangle_{l_1,l_2}. \tag{14}$$

The relations (11)–(14) are straightforward to implement numerically.

In the analysis of the form of the vortex lattice the parameter ν was considered to lowest order in perturbation theory (recall that $|\nu|\leq 1$ so that ν provides a natural expansion parameter). The limit $\nu=0$ was considered by Zhitomirsky who analytically found the ground-state eigenvector near H_{c_2}.[16] The solution of the order parameter to first order in ν is

$$(\eta_+,\eta_-)=[\phi_0+b_4\nu e^{-i4\theta}\phi_4,-e^{i2\theta}(\epsilon\phi_2+b_6\nu e^{-i4\theta}\phi_6)], \tag{15}$$

where $\epsilon=\sqrt{3}-\sqrt{2}\approx 0.317\,84$, $b_4=2\sqrt{3}\epsilon(10+\sqrt{6})/(36+16\sqrt{6})\approx 0.182\,30$, and $b_6=\sqrt{30}b_4/(10+\sqrt{6})\approx 0.080\,203$. Substituting this solution for the eigenstate near H_{c_2} into Eq. (7) yields the coefficients

$$(j_+)_{0,1}=1-\sqrt{2}\epsilon,$$

$$(j_+)_{0,5}=e^{i4\theta}\nu(\sqrt{5}b_4-\sqrt{6}b_6),$$

$$(j_+)_{1,2}=\sqrt{2}\epsilon^2-\epsilon,$$

$$(j_+)_{1,6}=e^{i4\theta}b_6\nu(\sqrt{2}\epsilon-1),$$

$$(j_+)_{2,3}=\sqrt{3}\epsilon^2,$$

$$(j_+)_{2,7}=e^{i4\theta}\sqrt{7}\epsilon b_6\nu,$$

$$(j_+)_{3,0}=e^{i4\theta}\nu(2b_4-\sqrt{3}\epsilon),$$

$$(j_+)_{4,1}=e^{-i4\theta}\nu b_4(1-\sqrt{2}\epsilon),$$

$$(j_+)_{5,2}=e^{-i4\theta}\epsilon\nu(\sqrt{6}b_6-\sqrt{5}b_4),$$

$$(j_+)_{6,3}=e^{-i4\theta}b_6\nu\sqrt{3}\epsilon.$$

Application of Eq. (8) yields

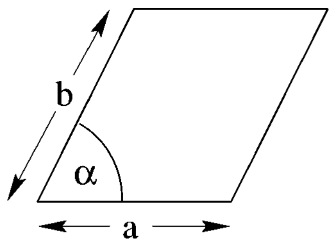

FIG. 2. The vortex lattice unit cell.

$$h_s = -h_{s0}[(1-3/\sqrt{2}\epsilon+2\epsilon^2)|\phi_0|^2+(2\epsilon^2-\epsilon/\sqrt{2})|\phi_1|^2 + \epsilon^2|\phi_2|^2+\nu[(\sqrt{10}\epsilon b_4/4-\sqrt{6}b_6/4)(e^{i4\theta}\phi_1^*\phi_5 + e^{-i4\theta}\phi_5^*\phi_1)+(\sqrt{30}\epsilon b_4/4-\epsilon b_6-\sqrt{2}b_6/4)(e^{i4\theta}\phi_2^*\phi_6 + e^{-i4\theta}\phi_6^*\phi_2)+(\sqrt{3}\epsilon/2-b_4)(e^{i4\theta}\phi_4^*\phi_0 + e^{-i4\theta}\phi_0^*\phi_4)], \tag{16}$$

where

$$h_{s0}=\frac{b\sin\alpha}{\sqrt{\pi}(1-2\sqrt{2}\epsilon+4\epsilon^2)}\frac{H_{c2}-H}{(2\tilde{\kappa}^2-1)\beta_A}. \tag{17}$$

Using this expression for h_s, $(2\tilde{\kappa}^2-1)\beta_A$ should be minimized with respect to θ, σ, and ρ to find the form of the vortex lattice. It can be proven when $\nu>0$ ($\nu<0$) $(2\tilde{\kappa}^2-1)\beta_A$ can be minimized for $\theta=\pi/4$ ($\theta=0$). For $\nu=0$, $(2\tilde{\kappa}^2-1)\beta_A$ is independent of θ. This is to be expected since $\nu=0$ corresponds to a cylindrically symmetric Fermi surface. It is also found that $\tilde{\kappa}$ varies weakly (≈ 0.01) for the different vortex lattice structures studied in this paper (such behavior is also present for mixed d- and s-wave order parameters[13]). While this variation is small it determines the form of the vortex lattice in the region of $\tilde{\kappa}\approx 1/\sqrt{2}$ and at small κ the vortex lattice phase diagram becomes quite rich.

The form of the vortex lattice found in the large κ limit agrees with that found under more restrictive assumptions in Ref. 8. In this limit the lattice structure depends upon ν. The behavior of the vortex lattice as a function of ν is similar to the behavior as a function of temperature found for borocarbide[17] and d-wave[18,13] superconductors. For $\nu=0$ a hexagonal lattice is found. As $|\nu|$ increases the lattice deforms continuously until $|\nu|=0.0114$. For $0<|\nu|<0.0114$ the vortex lattice is a centered rectangular lattice as shown in Fig. 3 (which can be described by $\theta=\pi/4-\alpha$, $\rho=\cos\alpha$, and $\sigma=\sin\alpha$ where $\pi/3<\alpha<\pi/2$, $\alpha=\pi/3$ corresponds to the hexagonal lattice and $\alpha=\pi/2$ to the square lattice). For $|\nu|\geqslant 0.0114$ the vortex lattice is square. If $\nu\geqslant 0.0114$ the vortex lattice is rotated $\pi/4$ with respect to the underlying crystal lattice while for $\nu\leqslant -0.0114$ the vortex lattice is aligned with the underlying crystal lattice.

As mentioned above when κ becomes sufficiently small the vortex lattice phase diagram becomes richer. Figure 3 shows the region of stability for the three vortex lattice states that were found to be stable. In addition to the two phases described above, a third phase appears for small κ. The vortex lattice for this phase has a rectangular unit cell and is described by $\rho=0$ and $\sigma=b/a$. This phase is stable because

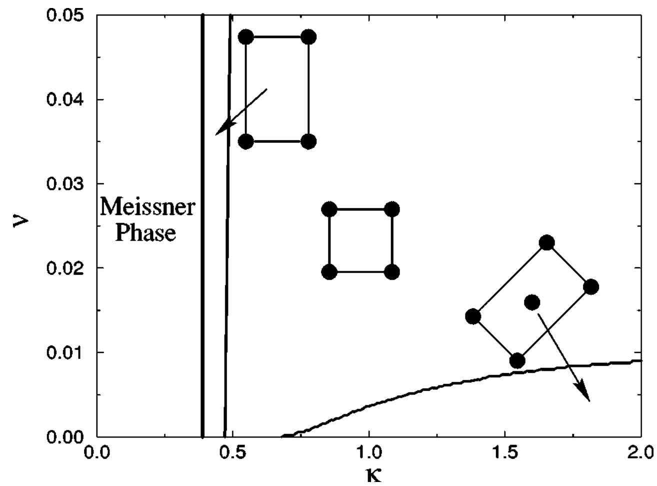

FIG. 3. The vortex lattice phase diagram as a function of the Ginzburg-Landau ratio κ and the square anisotropy parameter ν. The phase diagram is the same for $\nu<0$. For $\nu>0$ ($\nu<0$) the square vortex lattice is rotated $\pi/4$ (0) with respect to the underlying crystal lattice.

$\tilde{\kappa}$ is smaller for this phase than for both the square and hexagonal lattices. For a cylindrically symmetric Fermi surface ($\nu=0$) and $\kappa<0.75$ the hexagonal vortex lattice is no longer the stable structure. This arises because $\tilde{\kappa}$ is in a local maximum for the hexagonal lattice.

The type-I to type-II transition can also be determined and it is not given by $\tilde{\kappa}=1/\sqrt{2}$ but by $H_{c_2}=H_c$ (which corresponds to $\kappa=\epsilon\sqrt{3/2}$ up to corrections that are second order in ν). For a conventional superconductor $\tilde{\kappa}=1/\sqrt{2}$ and $H_{c_2}=H_c$ are equivalent. Here it is found that the κ for which $\tilde{\kappa}=1/\sqrt{2}$ is less than $\kappa=\epsilon\sqrt{3/2}$ for all lattice structures studied. An analysis of the Gibbs energies indicates that the Meissner state is the stable phase for H near H_{c_2} when $\kappa<\epsilon\sqrt{3/2}$.

Clearly, the square vortex lattice has the largest region of stability in Fig 3. To further investigate the square vortex lattice the spatial variation of the magnetic field as given by Eq. (16) is determined. This is shown in Fig. 4 for $\nu=0$ and for $\nu=0.2$. The induced field h_s has (in addition to a global maximum and a global minimum) a local minimum and a saddle point. Figure 5 shows the field distribution for these two values of ν as determined from

$$P(h)=\frac{\int d^2r\,\delta[h-h(\mathbf{r})]}{\int d^2r}. \tag{18}$$

The peak in $P(h)$ is due to the saddle point in the spatial dependence of h_s. As ν increases the saddle point value of h_s moves away from the minimum value of h_s resulting in a larger ''shoulder'' in $P(h)$ as ν increases.

Now I turn to an application of these results to Sr_2RuO_4. This requires a determination of the parameters ν and κ. The value of κ as defined above is given by

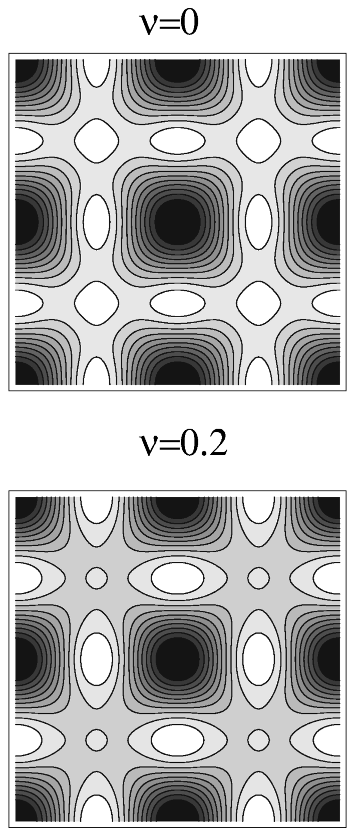

FIG. 4. Contour plots of the induced magnetic field h_s for a square vortex lattice with $\nu=0$ (top) and $\nu=0.2$ (bottom). The contours from darkest to lightest correspond to $\kappa h_s=-0.42\rightarrow -0.042$ in units 0.042.

$$\kappa=\frac{e_H\tilde{H}_{c_2}}{\sqrt{2}\tilde{H}_c}, \tag{19}$$

where e_H is given in Fig. 1 and $\tilde{H}_c$ ($\tilde{H}_{c_2}$) correspond to the measured critical (upper critical) field [note that the above choice of κ and ξ also implies $\tilde{H}_{c_2}=\Phi_0/(2e_H\pi\xi^2)$; also note that in Fig. 1 H_{c2} is in dimensionless units]. In principle, the values for $\tilde{H}_{c_2}$ and $\tilde{H}_c$ given in Ref. 19 can be used to estimate κ; however, the sample used had a $T_c=0.9$ K which indicates that impurities cannot be neglected (since $T_c^{max}\approx 1.5$ K) so that the clean-limit approximation used here is not valid. Until measurements on cleaner samples become available these measurements will be used to estimate κ. Using the values of $\tilde{H}_{c_2}=30$ mT and $\tilde{H}_c=17$ mT given in Ref. 19 yields $\kappa=1.2e_H<0.7$. This implies that either the square or the orthorhombic vortex lattices will occur depending on the value of ν.

To determine the value of ν experimentally the anisotropy of the upper critical field in the basal plane can be used,[20,8]

$$\frac{H_{c_2}(\mathbf{a})}{H_{c_2}(\mathbf{a}+\mathbf{b})}=\sqrt{\frac{1+\nu}{1-\nu}}, \tag{20}$$

where $H_{c_2}(\mathbf{a})$ $[H_{c_2}(\mathbf{a}+\mathbf{b})]$ is the upper critical field for the field along $\mathbf{a}$ $[\mathbf{a}+\mathbf{b}]$ measured at T_c. This anisotropy has not yet been determined so that a microscopic model must be used to estimate ν. Local-density approximation band-structure calculations[21,22] reveal that the density of states near the Fermi surface is due mainly to the four Ru $4d$ electrons in the t_{2g} orbitals. There is a strong hybridization of these orbitals with the O $2p$ orbitals giving rise to antibonding π^* bands. The resulting bands have three quasi-2D Fermi surface sheets labeled α, β, and γ (see Ref. 23). The α and β sheets consist of $\{xz,yz\}$ Wannier functions and the γ sheet of xy Wannier functions. In general, ν is not given by a simple average over all the sheets of the Fermi surface. A knowledge of the pair scattering amplitude on each sheet and between the sheets is required to determine ν.[10,11] It has been shown that the pair scattering amplitude between the γ and the $\{\alpha,\beta\}$ sheets of the Fermi surface is expected to be small relative to the intrasheet pair scattering amplitudes if Sr_2RuO_4 is not an isotropic s-wave superconductor.[10] This forms the basis for the model of orbital-dependent superconductivity in which, to account for the large residual density of states observed in the superconducting state, it has been proposed that either the xy or the $\{xz,yz\}$ Wannier functions exhibit superconducting order. This model implies that there are two possible values of ν; one for the γ sheet (ν_{xy}) and one for an average over the $\{\alpha,\beta\}$ sheets ($\nu_{xz,yz}$). Using the following tight-binding dispersions:

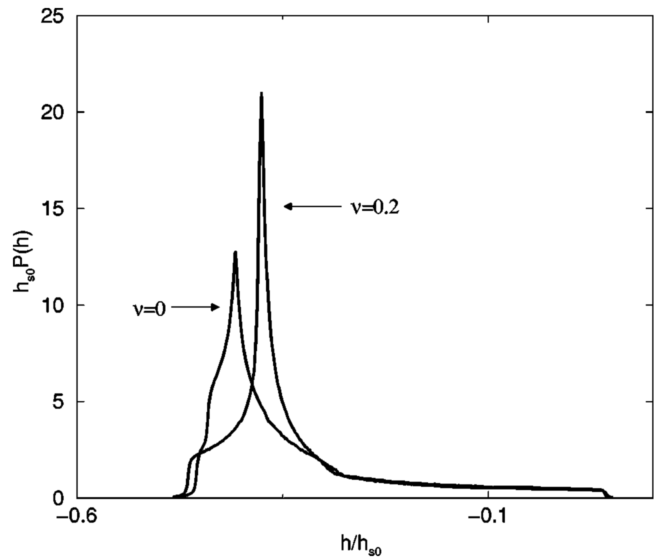

FIG. 5. Field distribution $P(h)$ near H_{c_2} for a square vortex lattice with $\nu=0$ and $\nu=0.2$.

$$\begin{aligned}\epsilon_\gamma&=\epsilon_\gamma^0-2t_\gamma(\cos k_x+\cos k_y)-4\tilde{t}_\gamma\cos k_x\cos k_y\epsilon_{\alpha,\beta}\\&=\epsilon_{\alpha,\beta}^0-2t_{\alpha,\beta}(\cos k_x+\cos k_y)\\&\quad\pm\sqrt{4t_{\alpha,\beta}^2(\cos k_x-\cos k_y)^2+16\tilde{t}_{\alpha,\beta}^2\sin^2k_x\sin^2k_y}\end{aligned} \tag{21}$$

and using the tight-binding values of Ref. 11 for the γ sheet $(\epsilon_\gamma^0,t_\gamma,\tilde{t}_\gamma)=(-0.4,0.4,0.12)$ and the values $(\epsilon_{\alpha,\beta}^0,t_{\alpha,\beta},\tilde{t}_{\alpha,\beta})=(-0.3,0.25,0.075)$ for the $\{\alpha,\beta\}$ sheets yields $\nu_{xy}=-0.6$ and $\nu_{xz,yz}=0.6$. These values of ν seem too large since they imply an anisotropy of a factor of 4 in $H_{c_2}(\mathbf{a})/H_{c_2}(\mathbf{a}+\mathbf{b})$. However, ν depends strongly upon the tight-binding parameters used; for example, taking $(\epsilon_\gamma^0, t_\gamma, \tilde{t}_\gamma) = (-0.52, 0.4, 0.16)$ yields $\nu_{xy} = -0.08$. The qualitative result that $\nu_{xy} < 0$ and $\nu_{xz,yz} > 0$ is robust. Physically $\nu_{xy} < 0$ because of the proximity of the γ Fermi surface sheet to a Van Hove singularity and $\nu_{xz,yz} > 0$ due to the quasi-1D nature of the $\{\alpha, \beta\}$ surfaces.[21,22] Assuming $|\nu| < 0.2$ implies $\kappa \approx 0.7$ [since $e_H = 0.5505 + O(\nu^2)$] in which case there will be a square vortex lattice that is rotated $\pi/4$ (0) with respect to the underlying crystal lattice if the pairing occurs on the $\{\alpha, \beta\}$ (γ) Fermi sheets. It is encouraging that Riseman *et al.* have observed a square vortex lattice in Sr_2RuO_4.[9] Further experimental studies of the vortex lattice should provide useful information as to the nature of the superconducting phase.

In conclusion, a Ginzburg-Landau theory for a two-component order parameter representation of the tetragonal point group has been examined with a magnetic field applied along the c axis. The vortex lattice phase diagram near H_{c_2} was found to be rich with a square vortex lattice occupying most of the parameter space. The field distribution of the square vortex lattice was determined yielding predictions for μSR measurements. Finally, the application of this model to Sr_2RuO_4 indicates that a square vortex lattice is expected to appear. The orientation of the square vortex lattice with respect to the underlying crystal lattice yields information as to which of the Ru $4d$ orbitals are relevant to the superconducting state.

I acknowledge support from the Natural Sciences and Engineering Research Council of Canada and the Zentrum fur Theoretische Physik. I wish to thank E.M. Forgan, R. Heeb, G. Luke, A. Mackenzie, Y. Maeno, T.M. Rice, M. Sigrist, and J. Sonier for useful discussions.

[1] Y. Maeno, H. Hashimoto, K. Yoshida, S. Nishizaki, T. Fujita, J. G. Bednorz, and F. Lichtenberg, Nature (London) **372**, 532 (1994).

[2] K. Ishida, Y. Kitaoka, K. Asayama, S. Ikeda, S. Nishizaki, Y. Maeno, K. Yoshida, and T. Fujita, Phys. Rev. B **56**, 505 (1997).

[3] A. P. Mackenzie, R. K. W. Haselwimmer, A. W. Tyler, G. G. Lonzarich, Y. Mori, S. Nishizaki, and Y. Maeno, Phys. Rev. Lett. **80**, 161 (1998).

[4] R. Jin, Yu. Zadorozhny, Y. Liu, Y. Mori, Y. Maeno, D. G. Schlom, and F. Lichtenberg, J. Chem. Phys. Solids (to be published).

[5] G. M. Luke, Y. Fudamoto, K. M. Kojima, M. I. Larkin, J. Merrin, B. Nachumi, Y. J. Uemura, Y. Maeno, Z. Q. Mao, Y. Mori, H. Nakamura, and M. Sigrist, Nature (London) **394**, 558 (1998).

[6] M. Sigrist and K. Ueda, Rev. Mod. Phys. **63**, 239 (1991).

[7] T. M. Rice and M. Sigrist, J. Phys.: Condens. Matter **7**, L643 (1995).

[8] D. F. Agterberg, Phys. Rev. Lett. **80**, 5184 (1998).

[9] T. M. Riseman, P. G. Kealy, E. M. Forgan, A. P. Mackenzie, L. M. Galvin, A. W. Tyler, S-L. Lee, C. Ager, D. Mck. Paul, C. M. Aegerter, R. Cubitt, Z. Q. Mao, S. Akima, and Y. Maeno, Nature (London) (to be published).

[10] D. F. Agterberg, T. M. Rice, and M. Sigrist, Phys. Rev. Lett. **78**, 3374 (1997).

[11] I. I. Mazin and D.J. Singh, Phys. Rev. Lett. **79**, 733 (1997).

[12] I. A. Luk'yanchuk and M. E. Zhitomirsky, Supercond. Rev. **1**, 207 (1995).

[13] M. Franz, C. Kallin, P. I. Solininen, A. J. Berlinsky, and A. L. Fetter, Phys. Rev. B **53**, 5795 (1996).

[14] K. Takanaka, Prog. Theor. Phys. **46**, 1301 (1071).

[15] D. Saint-James, G. Sarma, and E. J. Thomas, *Type II Superconductivity* (Pergamon Press, New York, 1969).

[16] M. E. Zhitomirskii, Pis'ma Zh. Eksp. Teor. Fiz. **49**, 333 (1989) [JETP Lett. **49**, 379 (1989)].

[17] Y. De Wilde, M. Iavarone, U. Welp, V. Metlushko, A. E. Koshelev, I. Aranson, G. W. Crabtree, and P. C. Canfield, Phys. Rev. Lett. **78**, 4273 (1997).

[18] M. Ichioka, N. Enomoto, and K. Machida, J. Phys. Soc. Jpn. **66**, 3928 (1997).

[19] K. Yoshida, Y. Maeno, S. Nishizaki, and T. Fujita, J. Phys. Soc. Jpn. **65**, 2220 (1996).

[20] L. I. Burlachkov, Zh. Eksp. Teor. Fiz. **89**, 1382 (1985) [Sov. Phys. JETP **62**, 800 (1985)].

[21] T. Oguchi, Phys. Rev. B **51**, 1385 (1995).

[22] D. J. Singh, Phys. Rev. B **52**, 1358 (1995).

[23] A. P. Mackenzie, S. R. Julian, A. J. Diver, G. J. McMullan, M. P. Ray, G. G. Lonzarich, Y. Maeno, S. Nishizaki, and T. Fujita, Phys. Rev. Lett. **76**, 3786 (1996).